Comparison of loads from HAWC2 and OpenFAST for the IEA Wind 15 MW Reference Wind Turbine

Jennifer Rinker[1], Evan Gaertner[2], Frederik Zahle[1], Witold Skrzypiński[1], Nikhar Abbas[2], Henrik Bredmose[1], Garrett Barter[2], Katherine Dykes[1]

[1]Department of Wind Energy, Technical University of Denmark, Roskilde, Denmark.
[2]National Wind Technology Center, National Renewable Energy Laboratory, Golden, CO, USA.

E-mail: `rink@dtu.dk`

Abstract.   Reference wind turbines (RWTs) that reflect the state-of-the-art of current wind energy technology are necessary in order to properly evaluate innovative methods in wind turbine design and evaluation. The International Energy Agency (IEA) Wind Technology Collaboration Platform (TCP) Task 37 has recently developed a new RWT geared towards offshore floating-foundation applications: the IEA Wind 15 MW. The model has been implemented in two aeroelastic codes, OpenFAST and HAWC2, based on an underlying common ontology. However, these toolchains result in slightly different structural parameters, and the two codes utilise different structural models. Thus, to increase the utility of the model, it is necessary to compare the aeroelastic responses. This paper compares aeroelastic loads calculated using different fidelities of the blade model in OpenFAST (ElastoDyn and BeamDyn) and HAWC2 (prismatic Timoshenko without torsion and Timoshenko with fully populated stiffness matrix), where both codes use the DTU Basic controller and the same turbulence boxes to reduce discrepancies. The aeroelastic responses to steady wind, step wind and turbulent wind (per IEC 61400-1 wind class IB) are considered. The results indicate a generally good agreement between the loads dominated by aerodynamic thrust and force, especially for the no-torsion blade models. Discrepancies were observed in other load channels, partially due to differences in the asymmetric loading of the rotor and partially due to differing closed-loop dynamics, and they will be the subject of future investigations.

1. Introduction
To successfully investigate the impacts of innovation on the efficacy and cost of wind energy systems, it is essential that well-tested, state-of-the-art reference wind turbines (RWTs) are shared publicly. On the one hand, commercial wind turbine models (even those out of production for many years) embody sensitive intellectual property information related to many system design aspects that cannot be shared publicly. On the other hand, sub-suppliers, developers, consultancies, and research institutes need models for wind turbines that closely resemble the commercial state-of-the-art in order to investigate scientific phenomena and innovative technologies that will help advance performance and reduce costs for next generation wind energy systems. One of the most well-known examples in wind energy is the National Renewable Energy Laboratory (NREL) 5 megawatt (MW) [1], but a large number of other RWTs have been produced to capture evolution in commercial technology over the years, including the Technical

University of Denmark (DTU) 10 MW [2] and the Wind Partnership for Advanced Component Technology (WindPACT) RWTs [3].

As the wind energy industry has developed, the need for new RWTs that reflect current and future technologies has grown. To this end, the International Energy Agency (IEA) Wind Technology Collaboration Platform (TCP) Task 37 on systems engineering has developed a series of RWTs [4]: the IEA Wind 3.4 MW RWT, the IEA Wind 10 MW RWT and recently the IEA Wind 15 MW, targeting offshore applications. The model was originally designed by researchers from the National Renewable Energy Laboratory (NREL) before being further developed collaboratively with researchers at the Technical University of Denmark (DTU). To maximize its utility, a variety of design documents and aeroelastic input files are provided on GitHub [5]. More information on the model specifications can be found in the design report [6].

The underlying definitions of the RWT are defined according to the IEA Wind Task 37 wind turbine ontology, windIO [7]—a formal, common definition of a wind turbine model—and this common ontology was converted to OpenFAST and HAWC2 implementations using different toolchains. DTU's toolchain used BECAS [8], HAWC2 [9] and HAWCStab2 [10], whereas NREL used Sonata/Anba4 [11], WISDEM [12], and OpenFAST [13, 14]. The differences in toolchains result in slightly different aeroelastic parameters, which will affect aeroelastic responses. To complicate matters, the implementations in both OpenFAST and HAWC2 have multiple blade models with different fidelities: OpenFAST has ElastoDyn and BeamDyn, and HAWC2 has prismatic Timoshenko without torsion, prismatic Timoshenko with torsion and a Timoshenko model with a fully populated stiffness matrix. For the IEA Wind 15 MW RWT to be useful to both industry and researchers, it is essential that its inter-code aeroelastic behavior is well understood. The most detailed source of information on differences between aeroelastic codes is the set of reports from the Offshore Code Comparison projects (OC3 [15], OC4 [16] and OC5 [17]). However, these reports compare too many different aeroelastic codes and use an aeroelastic model of a much smaller wind turbine, so we cannot draw relevant conclusions about differences in the aeroelastic response of the IEA Wind 15 MW. Thus, this paper seeks to provide a baseline inter-code comparison for the RWT, to yield key insights into the aeroelastic performance of ElastoDyn, BeamDyn and HAWC2 and to provide a case study in using windIO for collaborative research.

The remainder of the paper is organised as follows. Section 2 describes the considerations taken to reduce discrepancies in the blade structure, turbulence and controller. Comparisons of the blade natural frequencies and steady-state, step-wind and turbulent responses are provided in Sec. 3. Finally, the conclusions are drawn in Sec. 4.

2. Model comparisons

This section provides details on the modelling methodology, including particular efforts that were made to reduce discrepancies between the two models. The version of the IEA Wind 15 MW used in both OpenFAST and HAWC2 was the monopile model, but both hydrodynamics and the monopile flexibility were disabled to mimic an onshore turbine. The remaining subsections discuss specific aspects of the aerodynamics, blade structural modelling, turbulence modelling and controller that could cause discrepancies and what measures were taken to reduce those discrepancies.

2.1. Aerodynamics

The two aeroelastic codes use similar methodologies to calculate aerodynamic loading. The OpenFAST model uses AeroDyn to calculate the aerodynamic forces. Tower shadow is modeled using the baseline potential flow model and the unsteady airfoil aerodynamics are calculated with the Beddoes-Leishman model. The HAWC2 model uses its standard potential tower shadow model and a modified Beddoes-Leishman model for unsteady airfoil aerodynamics [18]. Both

models use Blade Element Momementum Theory, including empirical corrections like the Prandtl tip loss model.

2.2. Blade structural models

Both OpenFAST and HAWC2 allow different modeling fidelities for the blade structure:

- **OpenFAST**
  - **ElastoDyn**. ElastoDyn uses Euler-Bernoulli beam theory with assumed modes, modelling the blades as straight, isotropic beams with limited geometric nonlinearities and only flapwise and edgewise bending deflections (no torsion).
  - **BeamDyn**. BeamDyn uses geometrically exact beam theory with Legendre spectral finite elements, which better models blades with geometric nonlinearities and large deflections. A model is defined using distributed 6×6 mass and stiffness matrices.

- **HAWC2**
  - **Prismatic Timoshenko, no torsion (H2-PTNT)**. HAWC2's default beam model is a prismatic Timoshenko beam, which allows both bending and torsional deflections. The H2-PTNT model disables torsion by setting the torsional stiffness to an arbitrarily large value.
  - **Prismatic Timoshenko (H2-PT)**. HAWC2's default beam model is a prismatic Timoshenko beam with both bending and torsional deflections.
  - **Timoshenko with fully populated matrix (H2-FPM)**. HAWC2 also allows the specification of a Timoshenko beam model with fully populated 6×6 stiffness matrices, allowing more complex blade designs such as bend-twist-coupled blades. The inertial properties are modelled according to the prismatic Timoshenko beam theory.

The BeamDyn and H2-FPM blade properties were calculated using Sonata/ANBA4 and BECAS, respectively, using the same underlying ontology [6]. Due to different reference axes, coordinate systems, and modeling assumptions in OpenFAST and HAWC2, the same 6×6 matrices cannot be used in both BeamDyn and H2-FPM. H2-PT and H2-PTNT properties were then extracted from the corresponding higher-fidelity structural model. ElastoDyn properties were determined using PreComp and pyFrame3dd, included in the WISDEM toolbox.

The aeroelastic results presented in this paper compare ElastoDyn with H2-PTNT and BeamDyn with H2-FPM. Because the focus of this paper is a comparison of the model behaviour in the two different aeroelastic codes and due to space constraints, results from the H2-PT model are not presented. However, the model was simulated and found to behave very closely to the H2-FPM model.

2.3. Turbulence

The default turbulence simulators for OpenFAST and HAWC2 use different modeling methodologies: OpenFAST uses the Kaimal spectrum with exponential coherence (KSEC), whereas HAWC2 uses the Mann model. The Mann model uses a three-dimensional spectral tensor that includes spatial correlation, whereas the KSEC model uses three one-dimensional spectra and a spatial coherence model. These differences in inflow generation could have significant impact on the aeroelastic results. Therefore, the turbulence boxes used in the HAWC2 simulations were converted to an OpenFAST-friendly format using PyConTurb [19] and then used as inflow for the ElastoDyn and BeamDyn simulations.

2.4. Controller

A significant potential source of discrepancy in the dynamical behaviour of the models is different controller logics. The default controller for the OpenFAST implementation of the RWT is

NREL's ROSCO (Reference Open Source Controller) [20, 21], whereas the HAWC2 model uses the DTU Basic Controller [22]. For a code-to-code comparison, it is essential that as many possible sources of discrepancy are removed from the comparison. Thus, for this paper, the DTU Basic controller was compiled and coupled with OpenFAST, and the same controller parameters were used for the corresponding OpenFAST and HAWC2 models. There are two sets of controller parameters, one for the models with torsion and one for the models without torsion. Thus, ElastoDyn and H2-PTNT used the same controller parameters, as did BeamDyn and H2-FPM. Both sets of controller parameters were tuned using HAWCStab2 v2.16a [**?**] with assumed partial-load poles (torque controller) and full-load poles (pitch controller) of 0.05 Hz, 70% critical, and 0.03 Hz, 70% critical, respectively. The controller parameters can be found in the input files on the RWT GitHub [5].

3. Results

This section presents the comparisons of the aeroelastic results from HAWC2/HAWCStab2 and OpenFAST. An analysis of the blade structural models is first presented in Sec. 3.1, which includes the natural frequencies and a selection of distributed structural properties. Then, Secs. 3.2, 3.3 and 3.4 compare the steady-state, step-wind and turbulent responses, respectively. All OpenFAST results were simulated using version 2.2, the HAWC2 results were simulated using version 12.8_1900 and the HAWCStab2 natural frequencies were generated using version 2.16a.

3.1. Comparison of blade structural models

We first present a basic comparison of the four blade models of interest to verify their implementations. Fig. 1 plots the distributed mass density, flapwise stiffness, edgewise stiffness and torsional stiffness of the models (torsional stiffness omitted for ElastoDyn and H2-PTNT models). The values for the BeamDyn and H2-FPM models were extracted from the corresponding diagonal values of the 6×6 matrices. As noted previously, slight differences between the models are expected due to differences in the methodologies used to convert the underlying ontology into the aeroelastic input files, but the overall agreement is quite good.
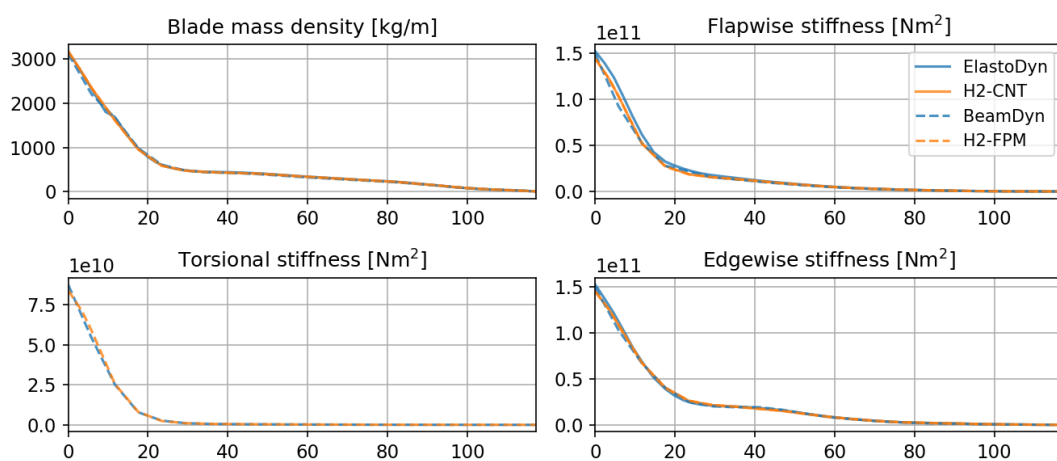

Figure 1. Comparison of distributed blade structural properties.

The structural natural frequencies of the blade calculated using OpenFAST's linearization option and HAWCStab2 [**?**] are compared in Table 1. The mode shapes were identified using HAWCStab2's mode-shape-visualization capabilities. The percent difference was calculated

Table 1. Blade structural natural frequencies in Hz (0 RPM).

Mode	ED	H2-PTNT	(% diff)	Mode	BD	H2-FPM	(% diff)
1st Flp	0.545	0.538	(1.2%)	1st Flp	0.517	0.521	(-0.8%)
1st Edg	0.631	0.638	(-1.0%)	1st Edg	0.630	0.619	(1.8%)
2nd Flp	1.618	1.658	(-2.4%)	2nd Flp	1.603	1.559	(2.8%)
2nd Edg	1.981	2.024	(-2.2%)	2nd Edg	1.964	1.933	(1.6%)
3rd Flp	3.239	3.385	(-4.4%)	3rd Flp	3.506	3.078	(13.0%)
3rd Edg	4.264	4.381	(-2.7%)	3rd Edg	4.403	4.156	(5.8%)
4th Flp	5.552	5.805	(-4.4%)	1st Trs	4.694	4.475	(4.8%)
4th Edg	7.160	7.439	(-3.8%)	4th Flp	5.307	5.056	(4.8%)

according to $p_{diff} = 2(f_{HAWC2} - f_{OpenFAST})/(f_{HAWC2} + f_{OpenFAST}) * 100\%$. The agreement between the two pairs of models (i.e., ElastoDyn vs. H2-PTNT and BeamDyn vs. H2-FPM) is generally good. This small differences in natural frequencies are a natural result of the difference in structural parameters, as discussed above. There is a larger difference in the 3rd flapwise mode in the BeamDyn/H2-FPM models, but it may be ignored in further analyses because it is sufficiently small and on a higher mode shape, which has a low modal participation factor in the overall response.

3.2. Steady state

Before considering the dynamical response of the turbine, it is important that we first compare the steady-state values (i.e., the mean aeroelastic response to steady wind). The steady values were calculates by running closed-loop, time-marching simulations in OpenFAST and HAWC2 with constant wind (no shear), removing the first part of the simulation to remove start-up effects and then taking the mean of the resulting aeroelastic response.

A selection of steady-state operational and aerodynamic values are given in Fig. 2. The models with torsion (ElastoDyn/H2-PTNT) are indicated by the solid lines, and those without torsion (BeamDyn/H2-FPM) are indicated by the dashed lines. The following observations may be made:

- **Good agreement in ElastoDyn and H2-PTNT operational data**. The steady-state generator speed, blade pitch, generator torque and generator power all have good agreement between the ElastoDyn and H2-PTNT models. This verifies that the slight differences in structural parameters do not significantly impact the controller set-points in OpenFAST and HAWC2.

- **Small differences in BeamDyn and H2-FPM operational data**. The structural differences between the BeamDyn and H2-FPM models are large enough to impact the controller set-points, as indicated by the differences in blade pitch angle, generator torque and generator power for the BeamDyn and H2-FPM models.

- **Small differences in ElastoDyn and H2-PTNT power coefficient (C_P) and thrust coefficient (C_T), but $C_{P,max} \approx C_{P,design}$.** There are slight differences between the C_P and C_T curves, as the OpenFAST calculation takes rotor deflection into account whereas the HAWC2 calculation does not. Regardless, the curves are quite similar, and the C_P value in Region 2 (optimal TSR) is near the design C_P value (0.489) [6].

- **Lower C_p and C_T for BeamDyn and H2-FPM models**. The C_P and C_T values for the models with torsion are generally lower, most notably in Region 2. This is indicative of the methodology used during the blade design, namely, that torsional deflection was not considered in the blade optimisation. Thus, the models with torsion will feature lower loads but also lower power generation.
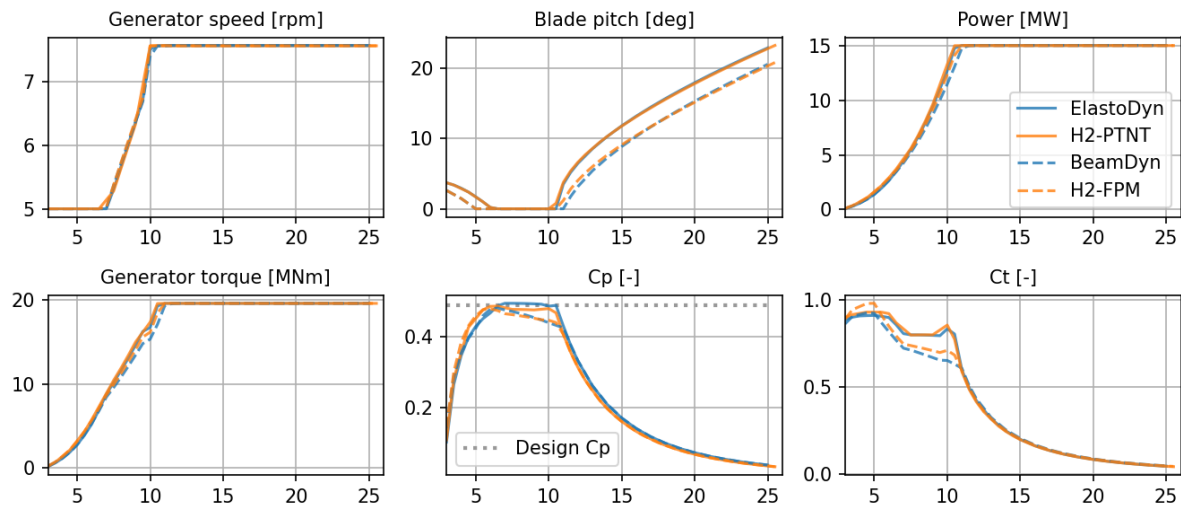
Figure 2. Comparison of steady-state operational and aerodynamic values.

A selection of steady-state loads and deflections are plotted in Fig. 3. From the plots, the following observations may be made:

- **Thrust- and torque-dominated loads for ElastoDyn and H2-PTNT match quite well**. The tower-base fore-aft moment, flapwise blade root moment and edgewise blade root moment are all loads that are primarily dominated by the aerodynamic thrust or aerodynamic torque. For the ElastoDyn and H2-PTNT models, the aerodynamic thrust and torque match quite well (not shown), and therefore these load channels also feature very good agreement.

- **Small differences in the thrust- and torque-dominated loads for the BeamDyn and H2-FPM models**. The differences in the BeamDyn and H2-FPM blade structural models and resulting difference in controller set-points result in thrust and torque curves for the BeamDyn and FPM models (not shown) that do not match as well as their no-torsion counterparts. These small differences in the thrust and torque curves for the BeamDyn and H2-FPM models then manifest as differences in the tower-base fore-aft moment, flapwise blade root moment and edgewise blade root moment. For example, the maximum flapwise blade root moment for BeamDyn is approximately 7.6% lower than H2-FPM.

- **Differences in the asymmetry-sensitive loads and deflections for all models**. The tower-base side-side moment and yaw-bearing pitch moment are both sensitive to asymmetric rotor loading, which is caused by tilt, coning, etc. These load channels demonstrate distinct differences not only between BeamDyn and H2-FPM but also ElastoDyn and H2-PTNT. Thus, there are differences in the net lateral and vertical force exerted on the rotor by the aerodynamic loading, which result in different tower-base side-side and yaw-bearing pitch moment values. This difference in the net lateral and vertical rotor loading could be caused by the difference in blade deflections (Fig. 3 bottom right subplot) or by fundamental differences in the aerodynamic calculations.

3.3. Step wind

The closed-loop dynamic response of the IEA Wind 15 MW simulated in HAWC2 and OpenFAST is given in Fig. 4. The step wind ranges from 3 to 25 m/s, and each step is 40 s long. An initial 220 s was added at the beginning of the simulation to ensure that any transient
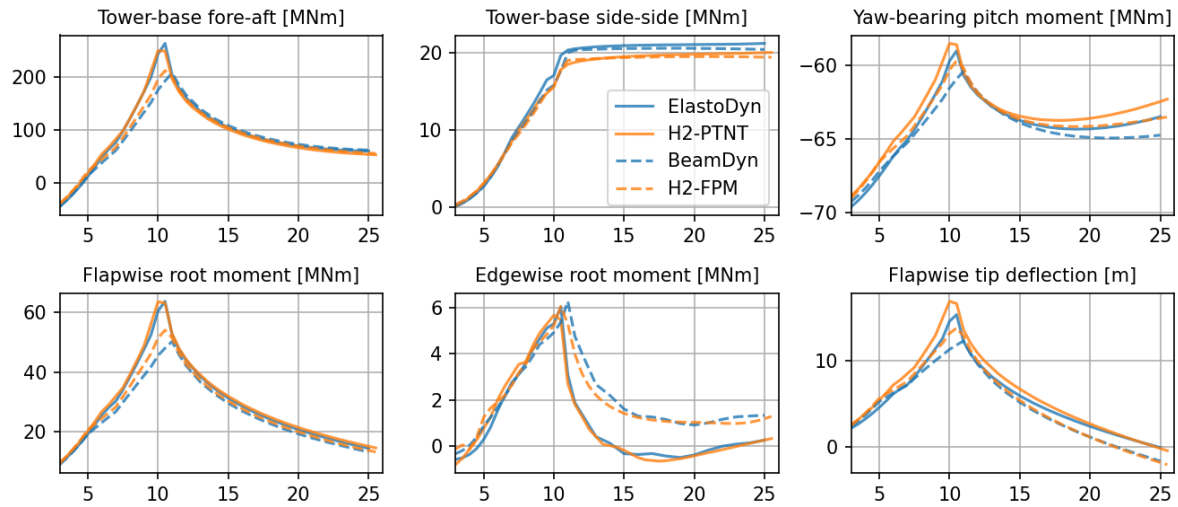
Figure 3. Comparison of steady-state loads and deflections.

behaviour from the start of the simulation has died out. The Region 1 wind speeds are from 220 to 300 s, Region 2 from 300 s to 540 and Region 3 from 540 s onwards.
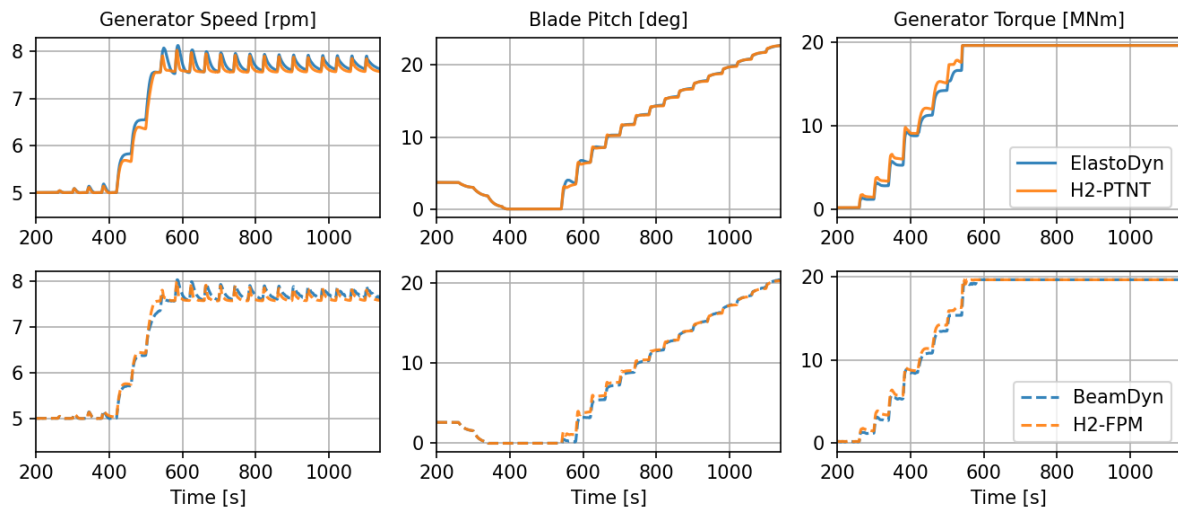

Figure 4. Step-wind response for OpenFAST (orange) and HAWC2 (blue).

The agreement between the two models is generally quite good, especially for the ElastoDyn/H2-PTNT models, with more discernible differences between the BeamDyn and H2-FPM responses. With the same controller and controller parameters between the two codes, the differences can be attributed to the structural modeling, both in terms of the structural property preprocessing and differences in the theoretical basis of the two codes. The resulting blade deflections and torsion also change the respective aerodynamic responses of the blades. Therefore, using the exact same controller parameters does not maximize agreement between the models. Minor re-tuning that accounts for the differences in the aeroelastic response is expected to further reduce discrepancies and will be the subject of future work. Generally though, the

difference in dynamics for these two models is small enough to be acceptable.

3.4. Turbulent wind

This section compares the aeroelastic responses for design load case (DLC) 1.1, as defined in the wind turbine design standard International Electrotechnical Commission (IEC) 61400-1 [23], wind class IB. 600-seconds turbulent simulations were run with mean wind speeds ranging from 3 to 25 m/s, in increments of 1 m/s, and the first 100 s were removed to eliminate transient behaviour. The presented results for the BeamDyn and H2-FPm models only include wind speeds up to 20 m/s due to a controller issue that forced shut-down during the transient start-up phase. The mean values and standard deviations are presented first, followed by the extreme values.
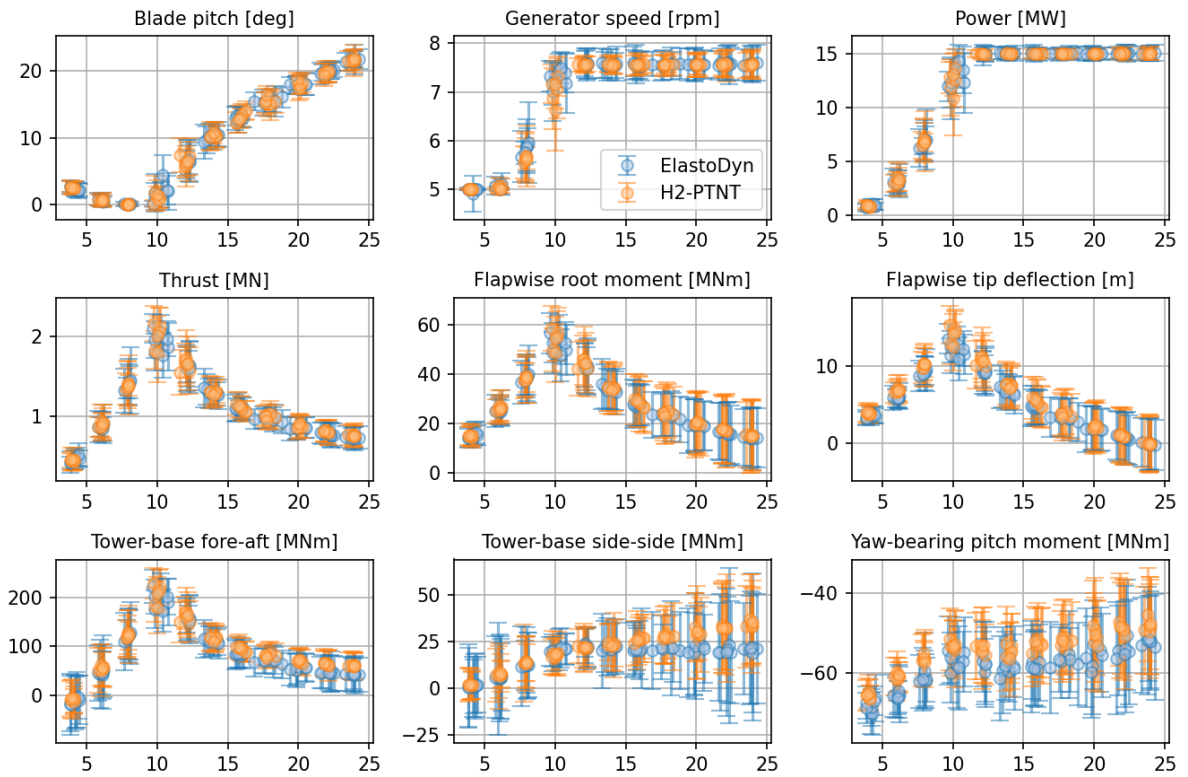
Figure 5. Mean (circles) and standard deviation (error bars) of aeroelastic response to class IB turbulence with H2-PTNT and ElastoDyn.

The statistics of a selection of load channels versus mean wind speed for ElastoDyn vs. H2-PTNT and BeamDyn vs. H2-FPM are presented in Figs. 5 and 6, respectively. The following observations may be made from the figures:

- **Good agreement in the operational data and thrust- and torque dominated channels for ElastDyn and H2-PTNT**. Because the rotor thrust and torque for the two models match quite well, the flapwise root moment and tower-base fore-aft have generally good agreement.

- **Higher thrust and related loads with H2-FPM**. Due to differences in the structural parameters, the H2-FPM model has a generally higher thrust than BeamDyn, which also
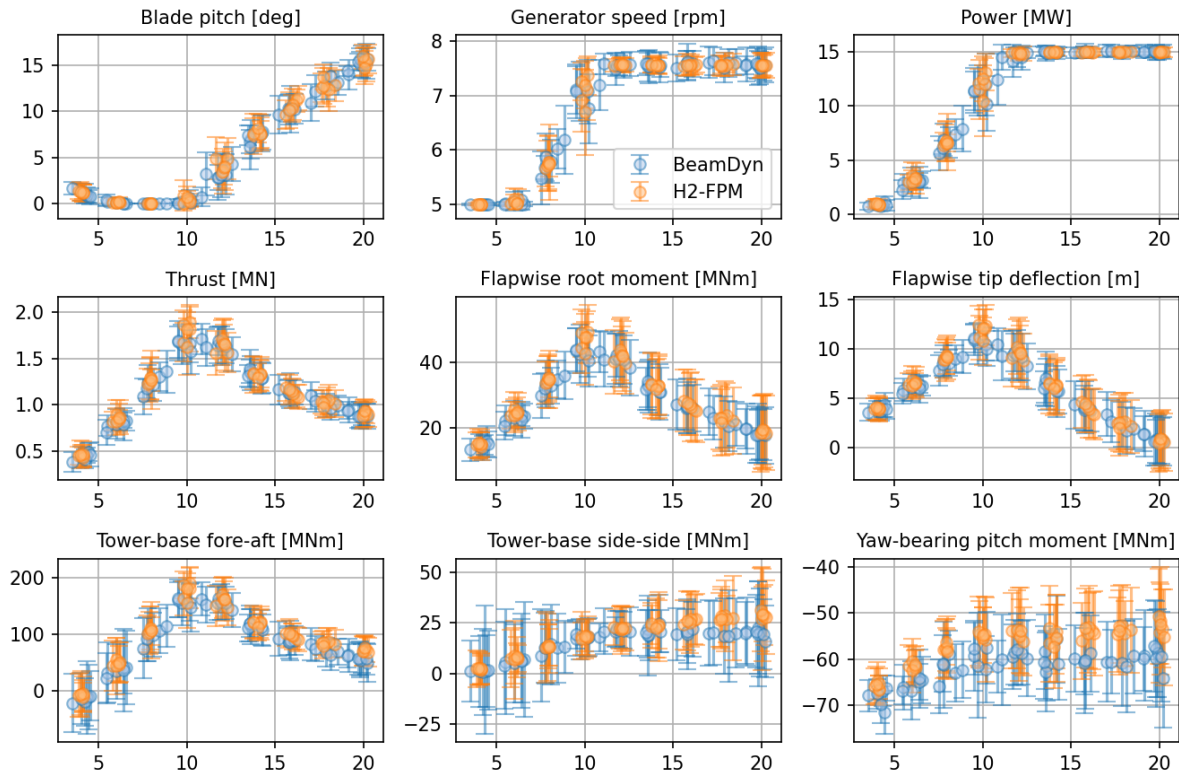
Figure 6. Mean (circles) and standard deviation (error bars) of aeroelastic response to class IB turbulence with H2-FPM and BeamDyn.

results in generally higher flapwise root moment, tip deflections and tower-base fore-aft moment.

- **Differences due to asymmetric rotor loading in all models**. Due to the addition of wind shear, there are larger differences between OpenFAST and HAWC2 due to asymmetric rotor loading. For example, for ElastoDyn vs. H2-PTNT, the mean yaw-bearing pitch moment and the mean tower-base moments at higher wind speeds show poor agreement. Similar trends are also seen in the BeamDyn vs. H2-FPM models.

- **Larger variation in OpenFAST tower-base moments at low wind speeds**. This is likely due to the controller parameters being ill-suited to the slightly different open-loop dynamics of the OpenFAST models. Future work could tune the controller parameters such that the OpenFAST and HAWC2 models demonstrated identical closed-loop behaviour.

The extreme values for ElastoDyn vs. H2-PTNT and BeamDyn vs. H2-FPM are presented in Figs. 7 and 8, respectively. From the plots, the following observations can be made:

- **Larger max generator speed and power in OpenFAST above rated**. This indicates that the identical controller parameters used in the two models do not produce the same closed-loop dynamics, resulting in larger OpenFAST overshoots. As noted above, future work could include a controller study that seeks to match the closed-loop behaviour of the two models.

- **Generally good agreement for ElastoDyn vs. H2-PTNT loads and deflections**. Except for the yaw-bearing pitch moment, the maximum values for the flapwise root moment, flapwise tip deflection and tower-base moments show generally good agreement.
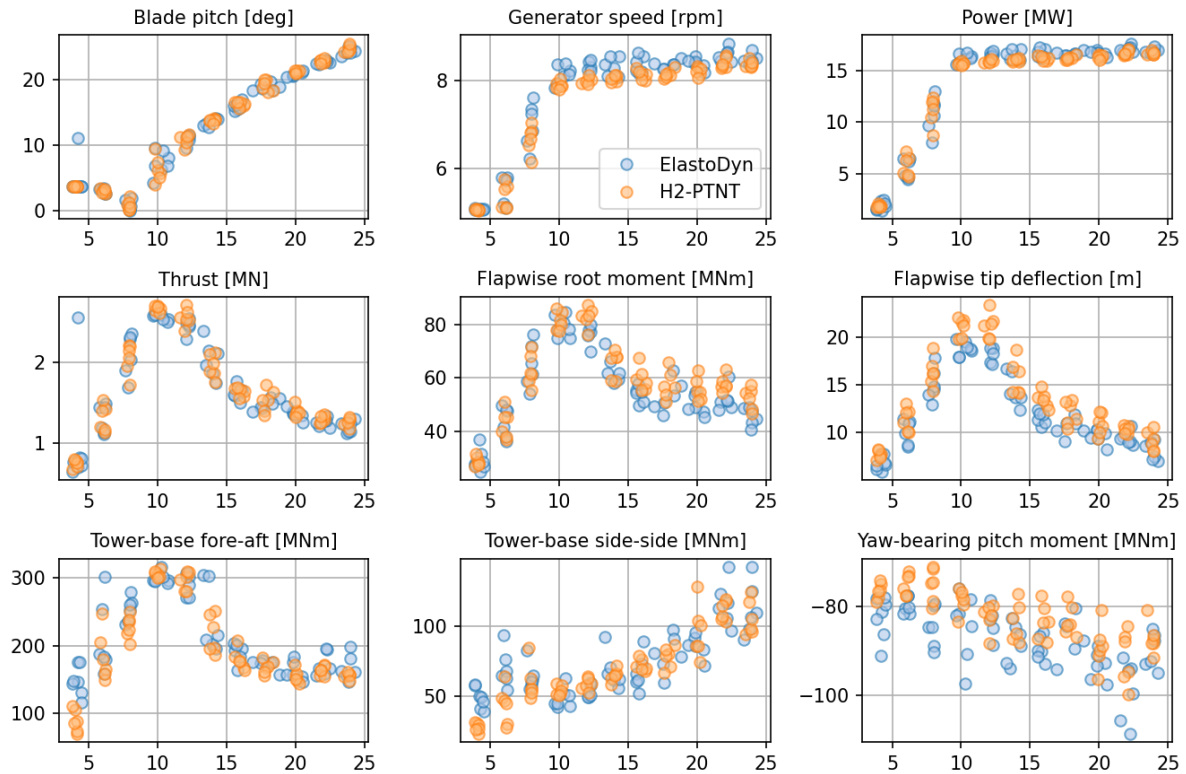
Figure 7. Extreme values of aeroelastic response to class IB turbulence with H2-PTNT and ElastoDyn.

As noted above, differences in the maximum yaw-bearing moment occur due to differences in the asymmetric rotor loading.

- **Larger maximum blade responses for H2-FPM than BeamDyn**. Because H2-FPM features larger mean thrust and torque than BeamDyn, the maximum values for the loads dominated by thrust and torque in H2-FPM are larger than their BeamDyn counterparts.

- **Relatively good agreement in tower-base loads for BeamDyn vs. H2-FPM**.

- **Similar maximum yaw-bearing pitch moment for BeamDyn vs. H2-FPM**. Considering that the mean value of the BeamDyn yaw-bearing pitch moment is more negative than the H2-FPM moment but their variations have similar amplitude, this might be indicative of suboptimal closed-loop behaviour. A future in-depth control study would be needed to examine this issue further.

4. Conclusions

This paper presents a detailed aeroelastic comparison of the IEA Wind 15 MW RWT as implemented in OpenFAST and HAWC2/HAWCStab2. The model was implemented in the two aeroelastic codes using separate toolchains, resulting in differences in structural properties, and it is important to quantify the effect these differences will have on the respective aeroelastic responses. To reduce the complexity of the analysis, particular efforts were made to reduce as many discrepancies between the two models as possible. First, two different HAWC2 models were used (Timoshenko without torsion and Timoshenko with a fully populated stiffness matrix) to better match the structural models used in ElastoDyn and BeamDyn, respectively. Second,
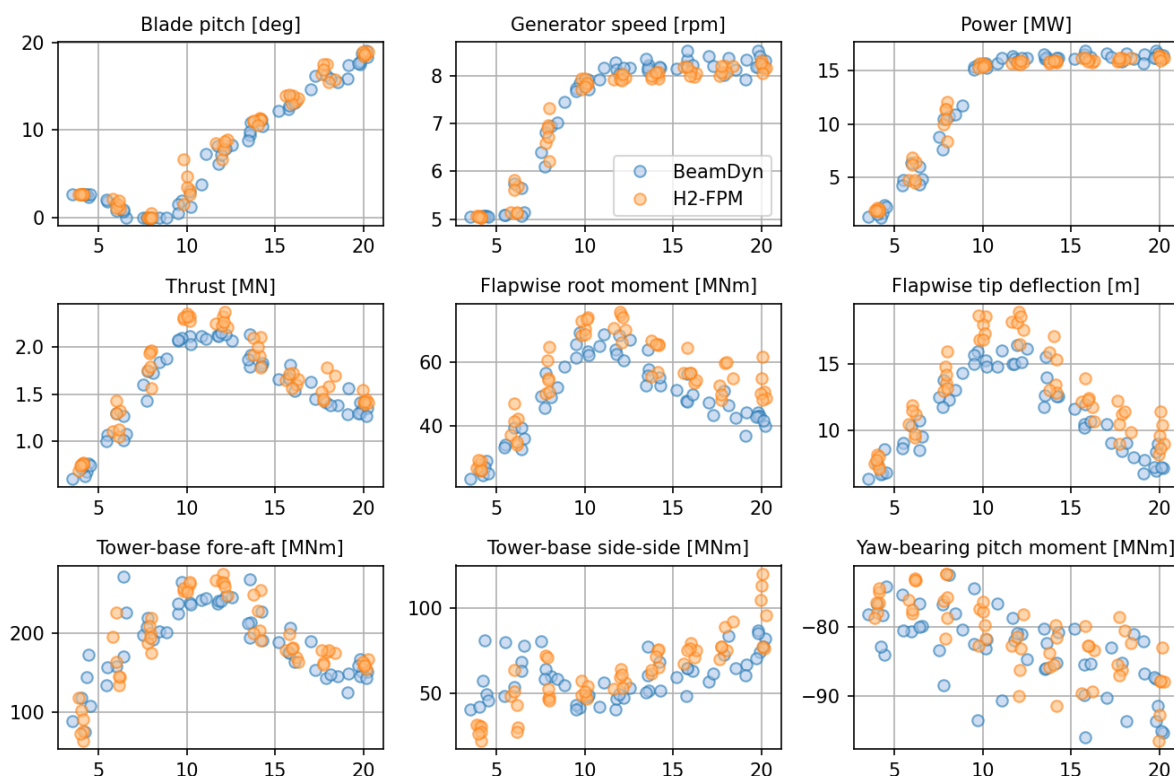
Figure 8. Extreme values of aeroelastic response to class IB turbulence with H2-FPM and BeamDyn.

the Mann turbulence boxes from HAWC2 were reused in OpenFAST to eliminate differences caused by inflow modelling. Lastly, the DTU Basic Controller with identical parameters was the controller in both models. The aeroelastic responses of the two pairs of models were evaluated by comparing their steady-state responses, step-wind responses and responses to turbulent wind prescribed according to IEC 61400-1 design load case 1.1.

The responses of all four models showed generally good agreement, although differences did arise that merit discussion. First, the load channels dominated by aerodynamic thrust and torque (e.g., tower-base bending moment) showed very good agreement between ElastoDyn and H2-PTNT. The differences in the structural values for BeamDyn and H2-FPM models resulted in higher aerodynamic thrust, so the loads dominated by thrust were slightly higher in the H2-FPM model. Interestingly, the load channels sensitive to asymmetric rotor loading (e.g., tower-base side-side moment and yaw-bearing moment) showed differences, even for the steady-state comparisons of ElastoDyn and H2-PTNT. Future work is needed to investigate whether this difference is caused by differences in the blade deflected shape of in the fundamental aerodynamics calculations. Lastly, although the same controller parameters were used in both aeroelastic codes, the differences in structural parameters resulted in different closed-loop behaviours. To remove this discrepancy, a future investigation must be made into tuning the controller parameters for a better agreement of the OpenFAST and HAWC2 closed-loop dynamics.

Despite the differences in certain responses, the results presented herein are of significant value to other scientists who are interested in the aeroelastic response of the IEA Wind 15-MW RWT. In particular, the use of the same turbulence boxes and the same controller sheds light

onto exactly how close the aeroelastic responses from the two codes can be. Thus, the results serve as an essential basis of comparison for future work that may utilize different controllers, turbulence models or other modifications to the models.

References

[1] Jonkman J M, Butterfield S, Musial W and Scott G 2009 Definition of a 5-MW reference wind turbine for offshore system development Tech. Rep. NREL/TP-500-38060 National Renewable Energy Laboratory Golden, CO

[2] Bak C, Zahle F, Bitsche R, Kim T, Yde A, Henriksen L C, Natarajan A and Hansen M H 2013 Description of the DTU 10 MW reference wind turbine Tech. Rep. I-0092 DTU Wind Energy

[3] Rinker J and Dykes K 2018 WindPACT reference wind turbines Tech. Rep. NREL/TP-5000-67667 National Renewable Energy Laboratory Golden, CO

[4] Bortolotti P, Tarrés H C, Dykes K, Merz K, Suthuraman L, Verelst D and Zahle F 2019 IEA wind TCP task 37: Systems engineering in wind energy - WP2.1 reference wind turbines Tech. rep. IEA Wind URL `https://www.nrel.gov/docs/fy19osti/73492.pdf`

[5] IEA Task 37 2020 IEA GitHub repository URL `https://github.com/IEAWindTask37/IEA-15-240-RWT`

[6] Gaertner E *et al* 2020 Definition of the IEA wind 15-megawatt offshore reference wind turbine Tech. Rep. NREL/TP-5000-75698 National Renewable Energy Laboratory Golden, CO

[7] IEA Wind Task 37 2020 windio documentation URL `https://windio.readthedocs.io/en/latest/`

[8] Blasques J 2012 User's manual for BECAS: A cross section analysis tool for anisotropic and inhomogeneous beam sections of arbitrary geometry Tech. Rep. Risø-R-1785 DTU Wind Energy Roskilde, Denmark

[9] Larsen T J and Hansen A M 2007 How 2 HAWC2, the user's manual Tech. Rep. Risø-R-1597 DTU Wind Energy Roskilde, Denmark

[10] Hansen M, Henriksen L, Tibaldi C, Bergami L, Verelst D, Pirrung G and Riva R 2018 HAWCStab2 User Manual Tech. rep. DTU Wind Energy Roskilde, Denmark

[11] Feil R, Pflumm T, Bortolotti P and Morandini M *Journal of Composite Structures* In review

[12] Dykes K, Graf P, Scott G, Ning A, King R, Guo Y, Parsons T, Damiani R, Felker F and Veers P 2015 Introducing WISDEM: An Integrated System Model of Wind Turbines and Plants URL `https://www.nrel.gov/docs/fy15osti/63564.pdf`

[13] Jonkman J and Buhl Jr M L 2005 FAST User's Guide Tech. Rep. NREL/EL-500-38230 National Renewable Energy Laboratory Golden, Colorado

[14] National Renewable Energy Laboratory 2019 OpenFAST Documentation URL `https://openfast.readthedocs.io/en/master/`

[15] Jonkman J and Musial W 2010 Offshore code comparison collaboration (OC3) for IEA task 23 offshore wind technology and deployment Tech. Rep. NREL/TP-5000-48191 National Renewable Energy Laboratory Golden, CO

[16] Popko W, Vorpahl F, Zuga A, Kohlmeier M, Jonkman J, Robertson A, Larsen T J, Yde A, Saetertro K and Okstad K M *et al* 2012 *22nd International Society of Offshore and Polar Engineers Conference* URL `https://www.nrel.gov/docs/fy12osti/54124.pdf`

[17] Robertson A N, Wendt F, Jonkman J M, Popko W, Dagher H, Gueydon S, Qvist J, Vittori F, Azcona J, Uzunoglu E *et al.* 2017 *Energy Procedia* **137** 38–57

[18] Hansen M H, Gaunaa M and Madsen H A 2004 A Beddoes-Leishman type dynamic stall model in state-space and indicial formulations Tech. Rep. Risø-R-1354 DTU Wind Energy

[19] Rinker J M 2018 *Journal of Physics: Conference Series* **1037** 062032

[20] National Renewable Energy Laboratory 2019 ROSCO Version 0.1.0 GitHub repository URL `https://github.com/NREL/rosco`

[21] Abbas N J, Wright A and Pao L 2020 vol 1452 (IOP Publishing) p 012002 URL `https://doi.org/10.1088%2F1742-6596%2F1452%2F1%2F012002`

[22] Hansen M H and Henriksen L C 2013 Basic DTU wind energy controller Tech. Rep. DTU Wind Energy E-0018 DTU Wind Energy Roskilde, Denmark

[23] International Electrotechnical Commission 2005 Wind turbines - part 1: design requirements 3rd ed.